

## 1 **Pervasive environmental chemicals impair oligodendrocyte development**

2  
3 Erin F. Cohn<sup>1</sup>, Benjamin L.L. Clayton<sup>1</sup>, Mayur Madhavan<sup>1</sup>, Sara Yacoub<sup>1</sup>, Yuriy Federov<sup>1</sup>, Katie  
4 Paul-Friedman<sup>2</sup>, Timothy J. Shafer<sup>2</sup>, Paul J. Tesar<sup>1\*</sup>

5  
6 <sup>1</sup>Department of Genetics and Genome Sciences, Case Western Reserve University School of  
7 Medicine, Cleveland, Ohio 44106, USA

8 <sup>2</sup>Center for Computational Toxicology and Exposure, Office of Research and Development, U.S.  
9 Environmental Protection Agency, Research Triangle Park, North Carolina 27711, USA

10  
11 \*email: paul.tesar@case.edu  
12  
13

### 14 **ABSTRACT:**

15 Exposure to environmental chemicals can impair neurodevelopment<sup>1-4</sup>. Oligodendrocytes that  
16 wrap around axons to boost neurotransmission may be particularly vulnerable to chemical toxicity  
17 as they develop throughout fetal development and into adulthood<sup>5,6</sup>. However, few environmental  
18 chemicals have been assessed for potential risks to oligodendrocyte development. Here, we  
19 utilized a high-throughput developmental screen and human cortical brain organoids, which  
20 revealed environmental chemicals in two classes that disrupt oligodendrocyte development  
21 through distinct mechanisms. Quaternary compounds, ubiquitous in disinfecting agents, hair  
22 conditioners, and fabric softeners, were potently and selectively cytotoxic to developing  
23 oligodendrocytes through activation of the integrated stress response. Organophosphate flame  
24 retardants, commonly found in household items such as furniture and electronics, were non-  
25 cytotoxic but prematurely arrested oligodendrocyte maturation. Chemicals from each class  
26 impaired human oligodendrocyte development in a 3D organoid model of prenatal cortical  
27 development. In analysis of epidemiological data from the CDC's National Health and Nutrition  
28 Examination Survey, adverse neurodevelopmental outcomes were associated with childhood  
29 exposure to the top organophosphate flame retardant identified by our oligodendrocyte toxicity  
30 platform. Collectively, our work identifies toxicological vulnerabilities specific to oligodendrocyte  
31 development and highlights common household chemicals with high exposure risk to children that  
32 warrant deeper scrutiny for their impact on human health.

33 **MAIN:**

34 Humans are exposed to a plethora of environmental chemicals with unknown toxicity profiles. The  
35 developing central nervous system is particularly sensitive to environmental insults and chemical  
36 exposures can be especially harmful to children if they occur during critical periods of  
37 development<sup>1,2</sup>. For example, the heavy metals methylmercury and lead, as well as industrial  
38 chemicals such as polychlorinated biphenyls are known to disrupt brain development<sup>3,4</sup>. Chemical  
39 exposures may trigger pathogenesis or exacerbate underlying genetic factors<sup>7-9</sup>. Importantly, the  
40 prevalence of neurodevelopmental disorders including autism spectrum disorder and attention-  
41 deficit hyperactivity has increased<sup>10,11</sup>, however, genetic factors can account for less than half of  
42 cases<sup>2</sup>. Therefore, evaluating how environmental factors, including chemical exposures,  
43 contribute to or initiate neurodevelopmental disorders has become imperative.

44  
45 While neurons have been more thoroughly evaluated for their susceptibility to chemical  
46 toxicity<sup>12,13</sup>, non-neuronal or glial cells are also essential for normal brain function.  
47 Oligodendrocytes generate myelin, a requirement for efficient neuronal transmission, and provide  
48 metabolic trophic support to neurons which is essential for their function and longevity<sup>5,14</sup>.  
49 Conversely, impaired oligodendrocyte development or their loss results in significant cognitive  
50 and motor disability in genetic diseases such as Pelizaeus-Merzbacher disease, and in  
51 inflammatory diseases such as multiple sclerosis<sup>15-17</sup>. A few environmental chemicals including  
52 natural products and industrial compounds reportedly alter oligodendrocyte function<sup>18,19</sup>.  
53 However, the vast majority of chemicals present in the environment have not been evaluated for  
54 oligodendrocyte toxicity, in large part, due to prior challenges in capturing oligodendrocyte  
55 development at high purity and scale.

56  
57 Both oligodendrogenesis and myelination have wide windows of vulnerability for environmental  
58 chemical exposure in humans. Development of oligodendrocytes from oligodendrocyte progenitor  
59 cells (OPCs) occurs throughout the first two years of life, and myelination begins during fetal  
60 development, peaks in infancy and childhood, and continues into adolescence and adulthood<sup>6,20</sup>.  
61 Therefore, oligodendrocytes are not only vulnerable during fetal development but also long after  
62 birth. In this study, we developed a toxicity screening platform to assess 1,823 chemicals that  
63 belong to the rapidly expanding repertoire of environmental contaminants. We identified  
64 chemicals belonging to two classes commonly found in households that perturb oligodendrocyte  
65 development.

66  
67 **RESULTS:**

68 **Phenotypic screen for environmental chemicals that disrupt oligodendrocyte development**

69 Previously, we established methods to generate OPCs from mouse pluripotent stem cells  
70 (mPSCs) at the scale required for high-throughput screening efforts<sup>21-23</sup>. mPSC-derived OPCs  
71 reliably develop into oligodendrocytes over 3 days *in vitro*, providing a robust approach for  
72 identifying environmental chemicals that affect oligodendrogenesis. We screened a library of  
73 1,823 chemicals to assess their effects on development of OPCs into oligodendrocytes (Fig. 1a).  
74 This library contains diverse chemicals with the potential for human exposure, including industrial  
75 chemicals, pesticides, and chemicals that are of interest to regulatory agencies<sup>24</sup>. In a primary  
76 screen, we treated OPCs with chemicals at a concentration of 20  $\mu$ M and allowed  
77 oligodendrocytes to develop for 3 days before analysis. Toxicity screening during the OPC to  
78 oligodendrocyte developmental transition enabled us to identify both chemicals cytotoxic to

79 developing oligodendrocytes and chemicals that impede oligodendrocyte generation without  
80 being cytotoxic.

81  
82 We determined chemical cytotoxicity in oligodendrocytes by quantifying viable nuclei based on  
83 staining with 4',6-diamidino-2-phenylindole (DAPI) and considered chemicals cytotoxic that  
84 reduced viability by more than 30% compared to the negative control. We further classified the  
85 remaining non-cytotoxic chemicals based on whether they interfered with the development of  
86 oligodendrocytes from OPCs by immunostaining for the O1 antigen, which is exclusively  
87 expressed on maturing oligodendrocytes. We considered non-cytotoxic chemicals that reduced  
88 the percentage of O1-positive cells by greater than 50% to be inhibitors of oligodendrocyte  
89 development. Conversely, we considered chemicals that increased the percentage of O1-positive  
90 cells by more than 20% to be drivers of oligodendrocyte development (Fig. 1b,c, and Extended  
91 Data Fig. 1a,b). Of the 1,823 chemicals in the primary screen, more than 80% had no effect on  
92 oligodendrocyte development or cytotoxicity, 292 were identified as cytotoxic to developing  
93 oligodendrocytes, 49 inhibited oligodendrocyte generation, and 22 stimulated oligodendrocyte  
94 generation (Fig. 1b, and Supplementary Table 1).

95  
96 **Quaternary compounds are selectively and potently cytotoxic to oligodendrocyte**  
97 **development**

98 To validate cytotoxic hits from the primary screen we used a colorimetric MTS tetrazolium assay  
99 designed to assess cell viability by measuring metabolic activity (Fig. 1d). To identify chemicals  
100 with specific cytotoxicity to oligodendrocyte development, we compared cytotoxicity profiles of  
101 206 MTS-validated chemicals from the primary screen to both an in-house primary screen in  
102 mouse astrocytes, representing another glial subtype, and a public database from the US  
103 Environmental Protection Agency (EPA), that contains cytotoxicity data for many cell types but  
104 not glial cells (Fig. 1e and Extended Data Fig. 2b). Chemicals cytotoxic to oligodendrocyte  
105 development but non-cytotoxic to astrocytes were tested in 10-point dose response (40 nM to 20  
106  $\mu$ M), and used to calculate  $IC_{50}$  values for each chemical (Fig. 1e and Extended Data Fig. 2c).  
107 Finally, we ranked the top ten cytotoxic chemicals based on potency in developing  
108 oligodendrocytes, lack of cytotoxicity to astrocytes, and lack of potency in cytotoxicity assays  
109 using other cell types (Fig. 1e).

110  
111 Through computational analysis we identified a chemical structure, characterized by a central  
112 nitrogen with four alkyl groups (bond.quatN\_alkyl\_acylic), as the most enriched structural domain  
113 among chemicals cytotoxic specifically to oligodendrocytes. This bond defines 13 quaternary  
114 ammonium compounds in the 1,823 chemical library. The primary screen identified 9 of these  
115 chemicals as cytotoxic to oligodendrocyte development, four of which are found in the top 12  
116 cytotoxic hits, including methyltrioctylammonium chloride (Fig. 1f,g, and Supplementary Table 2).  
117 The most highly ranked oligodendrocyte cytotoxic chemical, tributyltetradecylphosphonium, a  
118 quaternary phosphonium compound, has similar structure and function to quaternary ammonium  
119 compounds<sup>25</sup>. Given that our primary screen and secondary validation assays utilized mPSC-  
120 derived oligodendrocytes, we next confirmed cytotoxicity for two of the top ranked cytotoxic hits  
121 on oligodendrocytes generated from primary OPCs isolated directly from mouse postnatal brain  
122 tissue. Both methyltrioctylammonium chloride and tributyltetradecylphosphonium chloride, the  
123 two most highly ranked quaternary ammonium and phosphonium compounds (quaternary  
124 compounds) were cytotoxic at 20  $\mu$ M to primary OPCs, resulting in greater than 80% reduction in  
125 cell viability (Extended Data Fig. 2d,e). Collectively, these data demonstrate that quaternary

126 compounds are cytotoxic to developing oligodendrocytes. While quaternary phosphonium  
127 compounds are an emerging class of disinfectants<sup>25</sup>, current human exposure to quaternary  
128 ammonium compounds is likely as they are widely used in cosmetic products and as disinfecting  
129 agents, an application that increased significantly due to the COVID-19 pandemic<sup>26</sup>.  
130

### 131 **Quaternary compounds activate the integrated stress response to induce apoptosis**

132 To identify the mechanism underlying quaternary compound cytotoxicity in developing  
133 oligodendrocytes, we performed RNA sequencing on cells treated for 4 hours with two quaternary  
134 compounds: tributyltetradecylphosphonium chloride and methyltrioctylammonium chloride. Gene  
135 set enrichment analysis (GSEA) revealed that quaternary compound exposure results in  
136 enrichment for hallmark gene sets involved in programmed cell death and the integrated stress  
137 response (ISR) (Fig. 2a,b, and Supplementary Table 3). The ISR is activated by diverse  
138 environmental stressors and if not resolved, can lead to cell death. We confirmed activation of the  
139 ISR by performing qPCR using C/EBP homologous protein (CHOP), as a canonical marker of  
140 ISR activation and mediator of ISR-induced apoptosis (Fig. 2c). To determine the mechanism of  
141 cell death following ISR activation, we screened small molecule inhibitors of multiple programmed  
142 cell death pathways. We found that only QVD-OPH, an inhibitor of apoptosis, was able to prevent  
143 cell death induced by exposure to quaternary compounds (Extended Data Fig. 2f). These data  
144 suggest that quaternary compounds initiate ISR-mediated apoptosis in developing  
145 oligodendrocytes.  
146

### 147 **Quaternary compounds are cytotoxic to human oligodendrocyte development in cortical 148 organoids**

149 To determine whether quaternary compounds could disrupt human oligodendrocyte development,  
150 we leveraged our human pluripotent stem cell (hPSC)-derived regionalized neural organoid model  
151 in which oligodendrogenesis and myelination are integrated with fundamental processes of  
152 prenatal cortical development<sup>27,28</sup>. We supplemented media with methyltrioctylammonium  
153 chloride and tributyltetradecylphosphonium chloride on day 60, a critical time point for  
154 oligodendrocyte development (Fig. 2d). After culturing organoids in the presence of quaternary  
155 compounds for 10 days, we harvested organoids for analysis. Given that cell density was  
156 maintained across all conditions we concluded that quaternary compounds are not broadly  
157 cytotoxic. However, in immunohistochemistry analysis using the oligodendrocyte lineage marker,  
158 SOX10, we documented a significant reduction in SOX10-positive OPCs and oligodendrocytes  
159 (Fig. 2e,f). These results suggest that quaternary compounds are cytotoxic to developing human  
160 oligodendrocytes in an *in vitro* model of early human brain development.  
161

### 162 **Organophosphate flame retardants arrest oligodendrocyte development**

163 Many toxicity screens evaluate cell viability as a single endpoint measure. However, our screening  
164 platform allowed us to both identify cytotoxic chemicals and evaluate whether non-cytotoxic  
165 chemicals affect an essential developmental transition. Of the 1,539 non-cytotoxic compounds  
166 identified in the primary screen, 71 altered oligodendrocyte development. The 22 chemicals  
167 identified as enhancers of oligodendrocyte development largely consisted of thyroid hormone  
168 receptor modulators which are well known to drive oligodendrocyte generation (Extended Data  
169 Fig. 3a)<sup>29</sup>. The remaining 49 chemicals inhibited oligodendrocyte development (Fig. 3a).  
170 Computational analysis of oligodendrocyte inhibitors revealed an enriched structure characterized  
171 by a central phosphate (bond.P.O\_phosphate\_alkyl\_ester) as a top enriched structure with the  
172 highest odds ratio (Fig. 3b, and Supplementary Table 2). This structure is found in three chemical



173 hits, tris(methylphenyl) phosphate (TMPP), tris(2,3-dibromopropyl) phosphate (TBPP), and  
174 tris(1,3-dichloro-2-propyl) phosphate (TDCIPP). These chemicals are all organophosphate esters  
175 that belong to a large class of compounds widely used as both pesticides and flame retardants  
176 (Fig. 3c, and Extended Data Fig. 3b). Of the 13 organophosphate flame retardants in the primary  
177 screen chemical library, 7 chemicals reduced the percentage of O1-positive oligodendrocytes.  
178 We tested the top 3 organophosphate flame retardants in 8-point dose response (30 nM to 20  
179  $\mu$ M) and used these data to generate IC<sub>50</sub> values (Fig. 3d, and Extended Data Fig. 3b). All three  
180 organophosphate flame retardants also inhibited the development of oligodendrocytes from  
181 mouse OPCs isolated directly from postnatal brain tissue (Extended Data Fig. 3c,d).

182  
183 To identify at which stage of oligodendrocyte maturation organophosphate flame retardants exert  
184 their effect, we cultured developing oligodendrocytes in the presence of TDCIPP, TMPP, and  
185 TBPP and assessed maturation over three days. In our toxicity screening platform  
186 oligodendrocyte development proceeds through successive stages characterized by expression  
187 of known maturation markers (Fig. 3e). Specifically, early oligodendrocytes express the antigen  
188 for O4, intermediate oligodendrocytes express the antigen for O1, and mature oligodendrocytes  
189 express myelin basic protein (MBP). When we assessed the effects of organophosphate flame  
190 retardants on oligodendrocyte generation using immunocytochemistry for early (O4+),  
191 intermediate (O1+), and mature (MBP+) oligodendrocytes, we detected a delay in acquisition of  
192 O4 expression, and decreased O1 and MBP expression relative to the vehicle (DMSO)-treated  
193 negative control at all time points (Fig. 3e-g, and Extended Data Fig. 3e,f). These results suggest  
194 that, mechanistically, organophosphate flame retardants arrest the initial progression of early  
195 oligodendrocytes to intermediate and mature oligodendrocytes.

196  
197 **TDCIPP inhibits oligodendrocyte development in human cortical organoids**  
198 Next, we used our human cortical organoid model to assess whether organophosphate flame  
199 retardants inhibit human oligodendrocyte development. After culturing organoids from day 60 to  
200 day 70 in the presence of TDCIPP, we collected samples for immunohistochemistry. In the  
201 presence of TDCIPP, an oligodendrocyte marker CC1 was significantly decreased (Fig. 4a,b).  
202 Importantly, we found that cell density was unchanged across conditions, suggesting that the  
203 deficit in mature oligodendrocytes is indeed a selective inhibition of oligodendrocyte development.  
204 Collectively, these results suggest that the presence of TDCIPP is sufficient to arrest human  
205 oligodendrocyte development.

206  
207 **TDCIPP exposure during childhood and adolescence is significantly associated with**  
208 **abnormal neurodevelopment**

209 Organophosphate flame retardants are widely used in common products including furniture,  
210 building materials, and electronics. Human epidemiological studies investigating potential links  
211 between exposure to organophosphate flame retardants and developmental neurotoxicity have  
212 largely focused on prenatal exposures<sup>30</sup>. However, given the prolonged period of  
213 oligodendrogenesis and myelination after birth, we asked whether postnatal neurodevelopment  
214 would be impacted by organophosphate flame retardant exposure throughout childhood and  
215 adolescence. To that end, we analyzed data from the US CDC's National Health and Nutrition  
216 Examination Survey (NHANES) to identify levels of childhood exposure to organophosphate  
217 flame retardants and associations between exposure and indicators of abnormal cognitive and  
218 motor development. The NHANES is a cross-sectional study designed to collect survey,  
219 laboratory, and examination data from a nationally representative sample of US children and

220 adults. Due to the complex study design, these data can be leveraged to make estimations,  
221 including associations between laboratory-measured exposures and adverse outcomes, that are  
222 representative to the entire US population.

223  
224 Previous work has shown that the urine metabolite bis(1,3-dichloro-2-propyl) phosphate (BDCIPP)  
225 can accurately estimate exposure to its parent compound, the organophosphate flame retardant  
226 TDCIPP<sup>31</sup>. In examining a population of US children 3-17 years of age surveyed between 2017  
227 and 2018 we found that BDCIPP was present in urine samples for 998 out of 1,009, or 98.9%, of  
228 children (Fig. 4c,d; Extended Data Fig. 4a). Additionally, the amount of creatinine-adjusted  
229 BDCIPP was significantly higher when compared to adults (Fig. 4e). These data indicate that a  
230 majority of children were exposed to TDCIPP at the time of the survey and may experience higher  
231 internal doses compared to adults.

232  
233 Using multivariable-adjusted logistic regression, we identified associations between high levels of  
234 urinary BDCIPP, and three neurodevelopmental measures: gross motor dysfunction, a need for  
235 special education, and a need for mental health services (Extended Data Fig. 4b). These  
236 outcomes have been previously used to evaluate neurocognitive and neuromotor function<sup>32,33</sup>.  
237 Furthermore, oligodendrogenesis and myelination play essential roles in memory, learning, motor  
238 function, and mental health<sup>34-37</sup>. Weighted logistic regression analyses accounted for the  
239 NHANES complex survey design and were adjusted for age, sex, race/ethnicity, urine creatinine,  
240 as well as socioeconomic confounders previously reported to be associated with each  
241 outcome<sup>32,33</sup>. Children in the highest quintile of urinary BDCIPP concentration had increased  
242 adjusted odds ratios for all three neurodevelopmental outcomes when compared to children in  
243 the lowest quintile of urine BDCIPP concentration. The fully adjusted odds ratios for children in  
244 the high BDCIPP concentration group were 2.7 (95% CI = 1.01-7.41) for special education, 4.6  
245 (95% CI = 1.79-12.10) for mental health treatment, and 6.0 (95% CI = 1.24-29.42) for gross motor  
246 dysfunction (Fig. 4f,g; Extended Data Fig. 4c). These results indicate that children with high  
247 exposure are between 2.7 and 6 times more likely to experience adverse neurodevelopmental  
248 outcomes, providing strong evidence of a positive association between organophosphate flame  
249 retardant exposure and abnormal neurodevelopment.

## 250 251 **DISCUSSION:**

252 Evaluation of chemical safety is essential for the protection of human health. Although the effects  
253 of the vast majority of environmental chemicals on the central nervous system are unknown, high  
254 throughput screening is a powerful tool to prioritize chemicals of concern based on their toxic  
255 effects to physiologically relevant neural cell types and identify environmental triggers of  
256 pathogenesis<sup>8,38</sup>. Because oligodendrocytes represent a unique and understudied cell population  
257 in developmental neurotoxicology, we developed a toxicity screening platform to interrogate over  
258 1,800 environmental chemicals for their effects on oligodendrocyte development. Through this  
259 approach, we identified chemicals from two classes that impede the generation of  
260 oligodendrocytes: quaternary compounds and organophosphate flame retardants.

261  
262 Quaternary compounds are common in personal care products, pharmaceuticals, and anti-static  
263 agents. Their prevalent use in disinfectants, including more than half of EPA-registered products  
264 for eliminating SARS-CoV-2, is a likely cause of increased human exposure, demonstrated by the  
265 doubling in blood levels of some quaternary ammonium compounds since before the COVID-19  
266 pandemic<sup>39,40</sup>. In our oligodendrocyte-specific cytotoxic hits, quaternary compounds as a class

267 were enriched, and in a 3-D model of human prenatal brain development, our data show that  
268 these chemicals are specifically cytotoxic to human oligodendrocytes. We report that quaternary  
269 compounds induce the integrated stress response in developing oligodendrocytes, resulting in  
270 CHOP accumulation and apoptosis. In genetic and inflammatory diseases, developing and  
271 regenerating oligodendrocytes are particularly sensitive to ER stress and subsequent prolonged  
272 activation of the integrated stress response in part due to the requirement of developing  
273 oligodendrocytes to produce large amounts of myelin proteins<sup>41</sup>. This sensitivity may underlie the  
274 specific toxicity of quaternary compounds and could initiate or exacerbate pathology in disease.

275  
276 In developing oligodendrocytes, the IC<sub>50</sub> values for quaternary compound toxicity are in the  
277 nanomolar range, similar to predicted blood concentrations for many quaternary ammonium  
278 compounds in children<sup>42</sup>. Furthermore, we evaluated concentrations as acute exposures;  
279 whereas chronic exposures to quaternary compounds spanning oligodendrocyte development  
280 could drive toxicity at even lower concentrations, given their capacity for bioaccumulation<sup>39</sup>. When  
281 considering *in vitro* cytotoxicity data in mouse and human oligodendrocytes and the potential risk  
282 for chronic exposure, the increased use of quaternary ammonium compounds raises significant  
283 health concerns for neurodevelopmental toxicity given the ability of quaternary ammonium  
284 compounds such as benzalkonium chlorides, found in everyday household disinfecting agents, to  
285 pass both the blood placental and the blood brain barriers<sup>43</sup>. We also report the cytotoxicity of one  
286 quaternary phosphonium compound, tributyltetradecylphosphonium chloride. Although  
287 quaternary phosphonium compounds are less common than their ammonium-based  
288 counterparts, they have similar structure and function and may also have increased exposure to  
289 humans as they become implemented to combat bacterial resistance seen with quaternary  
290 ammonium compounds<sup>25</sup>.

291  
292 The pervasive use of organophosphate flame retardants has contaminated the environment and  
293 increased human exposure, demonstrated by the detection of these chemicals in human blood,  
294 urine, breast milk, and cerebrospinal fluid<sup>44,45</sup>. We show that the organophosphate flame retardant  
295 TDCIPP arrests the development of mouse oligodendrocytes and inhibits oligodendrocyte  
296 generation in human cortical organoids at concentrations similar to estimated blood  
297 concentrations in children<sup>46</sup>. Our results and the likelihood of organophosphate flame retardant  
298 exposure in children raise potential health concerns as these chemicals may reach higher  
299 concentrations in cerebrospinal fluid than blood<sup>47</sup>.

300  
301 Human epidemiological studies that evaluate prenatal exposure to TDCIPP, have identified  
302 associations between maternal exposure and delayed cognitive development<sup>30</sup>. However, these  
303 studies focused on solely prenatal exposures. Therefore, the disruption of critical periods of  
304 oligodendrogenesis and myelination during neurodevelopment in infancy and childhood by  
305 organophosphate flame retardants has yet to be evaluated. We analyzed the US CDC's NHANES  
306 2017-2018 dataset to identify associations between childhood exposure to organophosphate  
307 flame retardants and abnormal neurodevelopmental outcomes. Our logistic regression analyses  
308 demonstrate that there are significantly increased odds ratios for children with the highest urinary  
309 BDCIPP concentrations for multiple abnormal cognitive and motor outcomes. Continued  
310 evaluation of organophosphate flame retardant exposure and direct measurements of white  
311 matter development in children would provide critical evidence that chemical-mediated  
312 perturbation of oligodendrocyte development influences abnormal cognitive and motor outcomes.  
313 Although organophosphate flame retardants are pervasive and human exposure is ubiquitous,

314 behavioral interventions are effective in reducing exposure to TDCIPP and could be considered  
315 to minimize potential risks to children<sup>48</sup>.

316

317 This work reveals toxicological sensitivities in the oligodendrocyte lineage to common household  
318 chemicals and raises potential health concerns for exposure to these chemicals. Continued  
319 experimental and epidemiological studies are required to determine the full impact of exposure to  
320 quaternary ammonium and phosphonium compounds and organophosphate flame retardants.  
321 Results from this study will contribute to the scientific foundation that will inform decisions about  
322 regulatory or behavioral interventions designed to reduce chemical exposure and protect human  
323 health.

324 **METHODS:**

325 **Induced pluripotent stem cell-derived OPC culture**

326 Mouse OPCs were differentiated from mouse induced pluripotent stem cells (iPSCs) as previously  
327 described<sup>21,49</sup>. Briefly, iPSCs were removed from an irradiated mouse embryo fibroblast feeder  
328 layer with 1.5 mg/mL collagenase type IV (ThermoFisher, 17104019), dissociated with 0.25%  
329 trypsin-EDTA (ThermoFisher, 25200056), and seeded at  $7.8 \times 10^4$  cells/cm<sup>2</sup> on Costar Ultra-Low  
330 attachment plates (Sigma, CLS3471). Cells were cultured in media allowing for the expansion  
331 and maturation of OPCs for 9 days. On day 10, media was switched to OPC medium, comprised  
332 of N2B27 base medium, supplemented with 20 ng/mL FGF-2 (R&D Systems, 233-FB-010), and  
333 20 ng/mL PDGF-AA (R&D Systems, 221-AA). N2B27 base medium consists of Dulbecco's  
334 Modified Eagle Medium/Nutrient Mixture F-12 (DMEM/F-12; ThermoFisher 11320033),  
335 supplemented with 1X B-27 Supplement (ThermoFisher, 17504044), 1X N-2 MAX Supplement  
336 (ThermoFisher, 17502048), 1X GlutaMAX Supplement (ThermoFisher, 35050079). OPC medium  
337 was used over three passages to enrich for OPCs. OPC biological replicates were generated from  
338 independent mouse iPSC lines. Mouse iPSC-derived OPCs were used for all experiments unless  
339 otherwise noted.

340

341 **Primary mouse OPC and astrocyte culture**

342 All animal procedures were performed in accordance with the National Institutes of Health  
343 Guidelines for the Care and Use of Laboratory Animals and approved by the Case Western  
344 Reserve University Institutional Animal Care and Use Committee. Timed-pregnant mice  
345 (C57BL/6N) were ordered from Charles River (Wilmington, MA). Brains from mice were grossly  
346 dissected at postnatal day 2 (P2). Cortex tissue was isolated and dissociated using the Miltenyi  
347 Tumor Dissociation Kit (Miltenyi, 130-095-929) following the manufacturer's instructions.  
348 Following dissociation, cells were plated in poly-L-ornithine (Sigma, P3655) and laminin (Sigma,  
349 L2020) coated flasks and cultured for 24 hours. Culture media consists of N2B27 base medium  
350 supplemented with 20 ng/mL FGF-2 (R&D Systems, 233-FB-010), and 50 units/mL-50ug/mL  
351 Penicillin-Streptomycin (ThermoFisher, 15070063). After 24 hours of culture, media was switched  
352 to astrocyte or OPC enrichment media. OPC enrichment media is comprised of N2B27 base  
353 media supplemented with 20 ng/mL PDGF-AA (R&D Systems, 221-AA), 10ng/mL NT-3 (R&D  
354 Systems 267-N3), 100 ng/mL IGF (R&D Systems, 291-GF-200), 10  $\mu$ M cyclic AMP (Sigma,  
355 D0260), 100 ng/mL noggin (R&D Systems, 3344NG050) and 50 units/mL-50ug/mL Penicillin-  
356 Streptomycin (ThermoFisher, 15070063). OPCs were cultured in this media until the next  
357 passage, at which point 50 units/mL-50ug/mL Penicillin-Streptomycin was removed. Astrocyte  
358 enrichment media consists of 1:1 DMEM (ThermoFisher, 11960044)—Neurobasal Medium  
359 (ThermoFisher, 211-3-49), supplemented with 1X N-2 MAX Supplement (ThermoFisher,  
360 17502048), 1X GlutaMAX Supplement (ThermoFisher, 35050079), 50 units/mL-50ug/mL  
361 Penicillin-Streptomycin (ThermoFisher, 15070063), 5 ug/mL N-acetyl cysteine (Sigma, A8199),  
362 10 ng/mL CNTF (R&D 557-NT-010), 5 ng/mL HB-EGF (R&D Systems 259-HE-050), and 20  
363 ng/mL FGF-2 (R&D Systems, 233-FB-010). Media changes were performed every 48 hours and  
364 cells were allowed to proliferate, grown to confluency, and either passaged once or  
365 cryopreserved. For terminal experiments, astrocytes were thawed and plated into 384-well plates  
366 (Perkin Elmer, 6057500) at a density of 4,000 cells per well. Cells were then cultured with  
367 maturation media, comprised of 1:1 DMEM and Neurobasal media, supplemented with 1X N-2  
368 MAX, 5 ug/mL N-acetyl cysteine, 1X GlutaMAX Supplement, 1 mM Sodium Pyruvate  
369 (ThermoFisher, 11360-070), 5 ng/mL HB-EGF, 10 ng/mL CNTF, 50 ng/mL BMP4 (R&D, 314-BP-  
370 050) and 20 ng/mL FGF-2. After 48 hours of culture in astrocyte maturation media, cells were



371 cultured in resting astrocyte media (1:1 DMEM/Neurobasal Medium supplemented with 5 ng/mL  
372 HB-EGF) for 72 hours.

373

### 374 **Mouse oligodendrocyte differentiation**

375 OPCs were plated in 96-well plates (Fisher, 167008) coated with poly-L-ornithine (Sigma, P3655)  
376 and laminin (Sigma, L2020) at a seeding density of 40,000 cells per well, or 384-well plates coated  
377 with poly-D-lysine and laminin (Sigma, L2020) at a seeding density of 12,500 cells per well. Cells  
378 were plated in differentiation permissive media, comprised of Dulbecco's Modified Eagle  
379 Medium/Nutrient Mixture F-12 (DMEM/F-12; ThermoFisher 11320033), 1X B-27 Supplement  
380 (ThermoFisher, 17504044), 1X N-2 MAX Supplement (ThermoFisher, 17502048), 1X GlutaMAX  
381 Supplement (ThermoFisher, 35050079), 10ng/mL NT-3 (R&D Systems 267-N3), 100 ng/mL IGF  
382 (R&D Systems, 291-GF-200), 10  $\mu$ M cyclic AMP (Sigma, D0260), 100 ng/mL noggin (R&D  
383 Systems, 3344NG050), and 40 ng/mL T3 (Sigma, T6397) when noted. Cells were differentiated  
384 over 3 days and analyzed.

385

### 386 **Immunocytochemistry**

387 Live staining was performed for specific antigens (O1 and O4). Antibodies for O1 and O4 were  
388 diluted in N2B27 base medium supplemented with 5% Donkey Serum (v/v) (Jackson  
389 ImmunoResearch, 017-000-121) and added to wells for 18 minutes at 37°C. Cells were then fixed  
390 with 4% Paraformaldehyde (Electron Microscopy Sciences, HP1-100Kit) for 15 minutes at room  
391 temperature, washed with PBS, and incubated overnight at 4°C with primary antibody diluted in  
392 PBS supplemented with 5% Donkey Serum (v/v) and 0.1% Triton-X-100 (Sigma, T8787). Primary  
393 antibodies included anti-O1 (1:100, CCF Hybridoma core), anti-O4 (1:100, CCF Hybridoma core),  
394 and anti-MBP (1:4000, Abcam, ab7349). The following day cells were rinsed with PBS and  
395 incubated for 2 hours with the appropriate Alexa Fluor-conjugated secondary antibodies (2  $\mu$ g/mL,  
396 Thermo Fisher) and DAPI (1  $\mu$ g/mL, Sigma, D8417).

397

### 398 **Chemical screening**

399 Chemicals from the US EPA Toxicity Forecaster (ToxCast) chemical library were obtained  
400 through a Material Transfer Agreement with the US EPA. This library contained 1,823 chemicals  
401 dissolved in dimethyl sulfoxide (DMSO) at a top target stock concentration of 20 mM (with some  
402 chemicals achieving lower stock concentrations based on solubility limits in DMSO) and was  
403 stored at -20°C. Screening of the chemical library on OPCs was performed as described  
404 previously<sup>21</sup>. CellCarrier Ultra 384-well plates (PerkinElmer, 6057500), pre-coated with poly-D-  
405 lysine, were coated with laminin (Sigma, L2020) diluted in N2B27 base media, comprised of  
406 Dulbecco's Modified Eagle Medium/Nutrient Mixture F-12 (DMEM/F-12; ThermoFisher  
407 11320033), 1X B-27 Supplement (ThermoFisher, 17504044), 1X N-2 MAX Supplement  
408 (ThermoFisher, 17502048), and 1X GlutaMAX Supplement (ThermoFisher, 35050079). Laminin  
409 was dispensed using an EL406 Microplate Washer Dispenser (BioTek) using a 5  $\mu$ L dispense  
410 cassette (BioTek) and incubated for at least 1 hour at 37°C. OPCs were next dispensed in  
411 oligodendrocyte differentiation permissive media, at a density of 12,500 cells per well. OPCs were  
412 allowed to attach to the plates for 1 hour at 37°C and chemicals were added to plates at a 1:1000  
413 dilution using a Janus automated workstation and 50 nL solid pin tool attachment. Each  
414 compound was added at a final test well concentration of 20  $\mu$ M. Chemicals used for dose  
415 response validation were sourced from the primary screening library. DMSO (Sigma, D2650) was  
416 added at 1:1000 dilution to negative control wells and 40 ng/mL T3 (Sigma, T6397) was added to  
417 positive control wells. After 72 hours, cells were stained with anti-O1 (1:100, CCF Hybridoma

418 core), fixed with 4% Paraformaldehyde (Electron Microscopy Sciences, HP1-100Kit), and imaged  
419 using the Operetta High Content Imaging and Analysis system (PerkinElmer).

420

#### 421 **Kinetics of oligodendrocyte differentiation**

422 OPCs were seeded at a density of 40,000 cells per well in 96-well plates coated with in poly-L-  
423 ornithine (Sigma, P3655) and laminin (Sigma, L2020) in differentiation permissive media  
424 supplemented with 40 ng/mL T3 (Sigma, T6397). Cells were treated with TDCIPP (Sigma, 32951),  
425 TMPP (Santa Cruz, sc-296611), or TBPP (Millipore, 34188) at a final concentration of 20uM.  
426 DMSO (Sigma, D2650), was added at 1:1000 to negative control wells. As described previously<sup>50</sup>,  
427 cells were live stained with anti-O4 (1:100, CCF Hybridoma core), anti-O1 (1:100, CCF Hybridoma  
428 core), and fixed with 4% Paraformaldehyde (Electron Microscopy Sciences, HP1-100Kit) after 1-  
429 , 2-, and 3-days post-plating. Cells were then stained overnight with anti-MBP (1:4000, Abcam,  
430 ab7349) followed by staining with DAPI (1 µg/mL, Sigma, D8417). The Operetta High Content  
431 Imaging and Analysis system was used to image 4 fields per well and the percentage of O4, O1,  
432 and MBP-positive cells was quantified using the number of DAPI-positive live cells per field.

433

#### 434 **High content imaging and quantification**

435 The Operetta High Content Imaging and Analysis system was used to image all 96- and 384-well  
436 plates. For each well of the 96- and 384-well plates, 4 fields were captured at 20x magnification.  
437 The PerkinElmer Harmony and Columbus software was used to analyze images as described  
438 previously<sup>22,50,51</sup>. In brief, nuclei from live cells were identified by DAPI positivity, using  
439 thresholding to exclude cell debris or pyknotic nuclei. A region outside of each DAPI-positive  
440 nucleus, expanded by 50%, was used to identify oligodendrocytes by positive staining for  
441 oligodendrocyte markers (O1 in primary screen and O4, O1, or MBP in kinetics experiments)  
442 within this region. Expanded DAPI-positive nuclei that overlapped with O4, O1, or MBP staining  
443 were classified as oligodendrocytes. Cell viability was calculated by dividing the number of DAPI-  
444 positive nuclei in an experimental well by the average number of DAPI-positive cells in the  
445 negative control wells. Oligodendrocyte percentage was calculated by dividing the number of  
446 oligodendrocytes by DAPI-positive cells and normalized to negative control wells.

447

#### 448 **MTS assay**

449 OPCs were seeded at a density of 12,500 cells per well in CellCarrier Ultra 384-well plates  
450 (PerkinElmer, 6057500), pre-coated with poly-D-lysine and laminin (Sigma, L2020) in  
451 differentiation permissive media. Cells were allowed to attach for 1 hour at 37°C and compounds  
452 were added to plates at a 1:1000 dilution at a final concentration of 20 µM using a Janus  
453 automated workstation. DMSO (Sigma, D2650) was added at 1:1000 dilution to negative control  
454 wells and 40 ng/mL T3 (Sigma, T6397) was added to positive control wells. Cell viability was  
455 assessed after 72 hours using a 3-(4,5-dimethylthiazol-2-yl)-5-(3-carboxymethoxyphenyl)-2-(4-  
456 sulfophenyl)-2H-tetrazolium (MTS) assay kit (Abcam, ab197010) according to the manufacturer's  
457 protocol. Absorbance at 490 nm was measured 4 hours after the addition of the MTS dye using  
458 a SynergyNEO2 plate reader (BioTek).

459

#### 460 **Human cortical organoid production**

461 Human embryonic stem cell research was restricted to *in vitro* culture and *in vitro* cortical organoid  
462 generation using the human embryonic stem cell (hESC) line H7 (Wicell, WA07) and was  
463 performed following the International Society for Stem Cell Research 2021 Guidelines for Stem  
464 Cell Research and Clinical Translation. hESCs were expanded in mTesR1 media (Stem Cell

465 Technologies, 85850) and cortical organoids generated as previously described and with minor  
466 modifications<sup>27</sup>. Modifications include replacement of Y-27632 and dorsomorphin with CloneR  
467 (Stem Cell Technologies, 5889) and 150nM LDN193189 respectively during the first step in the  
468 generation of cortical organoids. For the first 6 days, organoids were cultured with media  
469 containing 10  $\mu$ M SB-43152 (Sigma, S4317) and 150 nM LDN193189, followed by 20 ng/mL EGF  
470 (R&D Systems, 236-EG-200) and 20 ng/mL FGF-2 (R&D Systems, 233-FB-010) on days 7 to 25.  
471 On days 27 to 40 organoids were fed on alternate days with media containing 20 ng/mL NT-3  
472 (R&D Systems, 267-N3) and 10 ng/mL BDNF (R&D Systems 248-BD). To expand OPC  
473 populations, 10 ng/mL PDGF-AA (R&D Systems, 221-AA) and 10 ng/mL IGF (R&D Systems,  
474 291-GF-200) were added to organoid cultures every other day between days 51 and 60. To induce  
475 the differentiation of oligodendrocytes 40 ng/mL T3 (Sigma, T6397) was added on alternate days  
476 between days 60 to 70. Organoids were treated with DMSO or chemicals beginning on day 60  
477 and harvested on day 70. Methyltrioctylammonium chloride and tributyltetradecylphosphonium  
478 chloride were sourced from the primary screening library and added at their IC<sub>90</sub> concentrations.  
479 TDCIPP (Sigma, 32951) was added at its approximate IC<sub>75</sub> concentration.

480

#### 481 **Cortical organoid immunohistochemistry**

482 Cortical organoids were treated on alternating days between days 61 to 70 with quaternary  
483 ammonium and phosphonium compounds or organophosphate flame retardants at their  
484 approximate IC<sub>90</sub> and IC<sub>75</sub> concentrations respectively. Organoids were harvested on day 70,  
485 washed in PBS, and fixed overnight with ice-cold 4% Paraformaldehyde (Electron Microscopy  
486 Sciences, HP1-100Kit). On the following day organoids were washed with PBS and cryoprotected  
487 using a 30% sucrose solution. Organoids were then embedded in OCT and sectioned at 15  $\mu$ M.  
488 Slides were washed with PBS and incubated overnight with anti-SOX10 (1:200, R&D, AF2864)  
489 and anti-APC CC1 (1:200, Millipore, MABC200), followed by labeling with Alexa Fluor-conjugated  
490 secondary antibodies (2  $\mu$ g/mL, Thermo Fisher). Slides were imaged at 10x magnification using  
491 a Hamamatsu Nanozoomer S60. Quantification of positive cells was performed using QuPath  
492 software (<https://qupath.github.io/>)<sup>52</sup>.

493

#### 494 **Cell death inhibitor testing**

495 OPCs were seeded in 384-well plates (PerkinElmer, 6057500) pre-coated with poly-D-lysine and  
496 laminin (Sigma, L2020) at a density of 12,500 cell per well and allowed to attach for 1 hour at  
497 37°C. Cell death inhibitors quinoline-Val-Asp-Difluorophenoxymethylketone (QVD-OPH) (Selleck,  
498 S7311), ferrostatin-1 (Selleck, S7243), and necrostatin-1 (Selleck, S8037), were added using a  
499 Janus automated workstation and 50 nL solid pin tool attachment in 8-point dose response (80  
500 nM to 10  $\mu$ M), and incubated for 1 hour at 37°C. Methyltrioctylammonium chloride or  
501 tributyltetradecylphosphonium chloride was added to all wells at IC<sub>90</sub> concentrations  
502 (approximately 100 nM), and oligodendrocytes were allowed to develop for 72 hours. Negative  
503 control wells contained only methyltrioctylammonium chloride or tributyltetradecylphosphonium  
504 chloride. Positive control wells contained vehicle (DMSO). Cells were fixed with 4%  
505 Paraformaldehyde (Electron Microscopy Sciences, HP1-100Kit) and stained with and DAPI (1  
506  $\mu$ g/mL, Sigma, D8417). Imaging was performed with the Operetta High Content Imaging and  
507 Analysis system (PerkinElmer) and the PerkinElmer Harmony and Columbus software was used  
508 to quantify DAPI-positive nuclei.

509

510

511

## 512 **RNA sequencing**

513 OPCs were plated in 6-well plates coated with poly-L-ornithine (Sigma, P3655) and laminin  
514 (Sigma, L2020) in OPC medium (Fisher Scientific, 14-832-11) and allowed to attach for one hour.  
515 OPCs were incubated with methyltrioctylammonium chloride and tributyltetradecylphosphonium  
516 chloride at their approximate IC<sub>90</sub> concentrations for 4 hours. OPCs were then lysed in TRIzol  
517 (Invitrogen, 15596018) and RNA was extracted by phenol-chloroform extraction and purified using  
518 the RNeasy Mini Kit (Qiagen, 74104). Samples were sent to Novogene for library preparation and  
519 mRNA sequencing. Libraries were generated according to protocols from the NEBNext Poly(A)  
520 mRNA Magnetic Isolation Module (NEB, E7490L) and NEBNext Ultra RNA Library Prep Kit for  
521 Illumina (NEB, E7530L) and then evenly pooled and sequenced on the Illumina NovaSeq with  
522 150bp paired-end reads and a read depth of at least 20 million reads per sample. Salmon 1.8.0.  
523 (<https://github.com/COMBINE-lab/salmon>)<sup>53</sup> was used to align reads to the mm10 genome and  
524 quantify transcript abundance as transcripts per million (TPM) values. The R package tximport  
525 was used to convert TPM values into gene-TPM abundance matrices.

526

## 527 **qRT-PCR**

528 OPCs were seeded at a density of 1,000,000 cells per well in poly-L-ornithine (Sigma, P3655)  
529 and laminin (Sigma, L2020) 6-well plates. OPCs were lysed using TRIzol (Invitrogen, 15596018)  
530 and RNA was isolated as described for RNA sequencing. RNA quantity and quality was assessed  
531 using a NanoDrop spectrophotometer and cDNA was synthesized using an iScript cDNA  
532 Synthesis Kit (Biorad, 1708891) following the manufacturer's instructions. qRT-PCR was  
533 performed using TaqMan gene expression assays (Thermo Fisher, 4369016) and run on an  
534 Applied Biosystems QuantStudio 3 real-time PCR system. *Rpl13a* (Mm05910660\_g1) was used as  
535 an endogenous control and probes for *Ddit3* (Mm01135937\_g1) were normalized to the  
536 endogenous control.

537

## 538 **Gene set enrichment analysis**

539 Gene set enrichment analysis (GSEA) software was used to calculate normalized enrichment  
540 scores, in hallmark datasets using 1000 gene-set permutations, classical scoring, and signal-to-  
541 noise metrics (<https://www.gsea-msigdb.org/gsea/index.jsp>). GSEA software generated  
542 normalized enrichment scores and false discovery rates. The integrated stress response gene  
543 set was curated from two published gene sets (Supplementary Table 3)<sup>54,55</sup>.

544

## 545 **US EPA ToxCast data**

546 Data from the US EPA ToxCast invitroDBv3.3, was used to assign use categories to chemical  
547 hits and obtain median cytotoxicity values. Chemical use categories were assigned based on  
548 "collected data on functional use" or "products use categories" obtained from the CompTox  
549 dashboard(<https://comptox.epa.gov/dashboard/>). Cytotoxicity median values were generated  
550 using data from the invitroDBv3.3 and the R package tcpl (ToxCast Analysis Pipeline)<sup>56</sup>.

551

## 552 **ToxPrint chemotype enrichment analysis**

553 ToxPrint chemotype enrichment analysis to identify enriched ToxPrints was performed as  
554 previously described using the publicly available ToxPrint feature set (<https://toxprint.org/>) and  
555 Chemotyper visualization application (<https://chemotyper.org/>)<sup>56</sup>. In separate analyses, chemical  
556 sets of interest were assigned as the "positive" chemical set and the remaining chemicals were  
557 assigned as the "negative" chemical set. Fischer's exact test was used to calculate p values for  
558 enriched ToxPrints in the positive chemical set compared to the negative set. Odds ratios were



559 calculated as described previously<sup>57</sup>. ToxPrints had a p value  $\leq 0.05$  and odds ratio  $\geq 3$  were  
560 considered significant and analyzed further.

561

### 562 **Statistical analysis**

563 GraphPad prism was used to perform curve-fitting for the calculation of IC<sub>50</sub>, IC<sub>75</sub> and IC<sub>90</sub> values  
564 and all statistical analyses unless otherwise specified. Data are typically presented as the mean  
565  $\pm$  standard deviation (SD) as described in figure legends. A p value  $\leq 0.05$  was considered  
566 statistically significant. For box-and-whisker plot, the box extends from 25<sup>th</sup> to 75<sup>th</sup> percentiles,  
567 with a line in the middle of the box at the median. Whiskers extend from the minimum to maximum  
568 values in the dataset.

569

### 570 **NHANES data source and study population**

571 Anonymized data from the National Health and Nutrition Examination Survey (NHANES) were  
572 downloaded from the US Centers for Disease Control and Prevention (CDC) website  
573 (<https://wwwn.cdc.gov/nchs/nhanes>). The 2017-2018 NHANES was approved by the CDC's  
574 National Center for Health and Statistics Ethics Review Board (protocol #2018-01) and is provided  
575 as anonymized data for public download. NHANES data were downloaded from the 2017-2018  
576 dataset and used for logistic regression analyses.

577

### 578 **NHANES exposure assessment**

579 Exposure to tris(1,3-dichloro-2-propyl) phosphate (TDCIPP) was assessed based on urinary  
580 concentrations of bis(1,3-dichloro-2-propyl) phosphate (BDCIPP). Levels of urine BDCIPP were  
581 measured in the 2017-2018 dataset in all children ages 3-5 years of age and a one-third subset  
582 of children ages 6-17 years of age. Detailed methods for the measurement of BDCIPP urine  
583 concentration are provided online via the NHANES website (<https://wwwn.cdc.gov/nchs/nhanes>).  
584 Briefly, BDCIPP concentration was determined by solid phase liquid extraction followed by isotope  
585 dilution-ultrahigh performance liquid chromatography-tandem mass spectrometry. The lower limit  
586 of detection (LLOD, in ng/mL) for this assay was 0.1. For analytes below the LLOD, an imputed  
587 fill value was generated by dividing the LLOD by the square root of 2.

588

### 589 **NHANES outcomes**

590 Three neurodevelopmental outcomes, including reported special education, gross motor  
591 impairment, and mental health treatment, were assessed. Children greater than or equal to 16  
592 years of age were interviewed directly. A proxy provided answers to questions for children below  
593 age 16 years of age. Proxies were asked the following questions to assess motor dysfunction:  
594 "Does Sample Person (SP) have an impairment or health problem that limits his/her ability to  
595 walk/run/play?". Children over the age of 16 were asked "Do you have an impairment or health  
596 problem that limits your ability to walk/run?" For assessment of special education utilization  
597 children and proxies were asked "Does SP receive Special Education or Early Intervention  
598 Services?". Determining whether a child required mental health services, children and proxies  
599 were asked "During the past 12 months, have you/has SP seen or talked to a mental health  
600 professional such as a psychologist, psychiatrist, psychiatric nurse, or clinical social worker about  
601 your/his/her health?"

602

### 603 **NHANES covariates**

604 NHANES collects data on other covariates including demographic and socioeconomic  
605 information. Subject age was determined based on participant's date of birth. Participant's gender



606 was queried at the time of the survey. Race/ethnicity was divided into five categories: Mexican  
607 American, other Hispanic, non-Hispanic white, non-Hispanic black, non-Hispanic Asian, other  
608 race-including multi-racial. Education level of the household reference person was split into three  
609 categories: less than high school degree, high school grad/GED or some college/AA degree, and  
610 college graduate or above. Poverty income ratios were calculated by dividing family income to  
611 poverty guidelines determined by the Department of Health and Human Services for the given  
612 survey year. Ratios at or above 5.00 were coded as 5.0. Department of Health and Human  
613 Services poverty guidelines were utilized to determine the ratio of family income to poverty.  
614 Detailed information on all NHANES covariates is available online  
615 (<https://www.cdc.gov/nchs/nhanes>).

616

### 617 **NHANES Statistical analysis**

618 All analyses were performed using SPSS. The complex samples logistic regression procedure in  
619 SPSS was used to perform multivariable-adjusted logistic regression to estimate adjusted odds  
620 ratios and 95% confidence intervals. All analyses specified strata, cluster, and environmental  
621 weight variables to account for the NHANES complex survey design. To assess the presence of  
622 non-linear relationships between urinary BDCIPP and neurodevelopmental outcomes, BDCIPP  
623 was evaluated in quintiles. We constructed two main models containing the following covariates:  
624 urinary creatinine, sex, age, race/ethnicity, ratio of family income to poverty, and education level  
625 of the household reference person. Age, urinary creatinine, and ratio of family income to poverty  
626 were modeled as continuous variables while sex, race/ethnicity, and education level of the  
627 household reference person were included as discrete covariates.

628

### 629 **DATA AVAILABILITY:**

630 Primary screening results are available in Supplementary Table 1 and will be included in the next  
631 public release of the US EPA ToxCast database. RNA-seq datasets generated in this study have  
632 been deposited in Gene Expression Omnibus (<https://www.ncbi.nlm.nih.gov/geo/>) under  
633 accession code GSE212190. Access key: qhwrmiisxdqvgd

634

### 635 **ACKNOWLEDGEMENTS:**

636 This work was supported by grants from the National Institutes of Health R35NS116842 (P.J.T.),  
637 F31NS124282 (E.F.C.), T32NS077888 (E.F.C.), and T32GM007250 (E.F.C.). B.L.L.C. is  
638 supported by a NMSS Career Transition Fellowship. Institutional support was provided by CWRU  
639 School of Medicine and philanthropic support was generously contributed by the Fakhouri, Long,  
640 Walter, Peterson, Goodman, and Geller families. Additional support was provided by the Small  
641 Molecule Drug Development and Light Microscopy Imaging core facilities of the CWRU  
642 Comprehensive Cancer Center (P30CA043703). The US Environmental Protection Agency  
643 provided the ToxCast screening library through MTA with CWRU and supported the effort of EPA  
644 employees (T.J.S. and K.P-F.). We are grateful to D. Adams, A. Wynshaw-Boris, K. Carr, K. Lee,  
645 J. Kristell, M. Scavuzzo, K. Allan, and A. Gartley for technical assistance and/or discussion.

646

### 647 **DISCLAIMER**

648 This work was supported in part by the US Environmental Protection Agency and has been  
649 reviewed and approved for publication by the US EPA's Center for Computational Toxicology and  
650 Exposure. Approval for publication does not signify that the contents reflect the views of the  
651 Agency, nor does mention of trade names or commercial products constitute an endorsement or  
652 recommendation for use.

653

654

655 **AUTHOR CONTRIBUTIONS:**

656 E.F.C., B.L.L.C., T.J.S., and P.J.T. conceived this study to screen effects of environmental  
657 chemicals on oligodendrocyte development. E.F.C., B.L.L.C., and P.J.T. designed and managed  
658 the experimental studies. E.F.C, B.L.L.C, and S.Y. performed, quantified, and analyzed in vitro  
659 experiments using mouse OPCs including primary screening, and immunocytochemistry. E.F.C.  
660 and S.Y. performed dose-curve validations and qPCR. B.L.L.C. isolated mouse astrocytes and  
661 performed primary screening for astrocytes. E.F.C. performed RNA-seq analysis. K.P-F  
662 performed ToxPrint chemotype enrichment analyses and T.J.S. and K.P.F. guided categorization  
663 of chemical screen hits. E.F.C. designed and performed linear regression analyses using data  
664 from the National Health and Nutrition Examination Survey. M.M. and E.F.C. performed cortical  
665 organoid experiments. Y.F. managed the chemical library and pipelined primary screening data.  
666 E.F.C assembled all figures. E.F.C. and P.J.T. wrote the manuscript with input from all authors.

667

668 **COMPETING INTERESTS:**

669 The authors declare no competing interests related to this work.

670

671 **REFERENCES:**

- 672 1. Grandjean, P. & Landrigan, P.J. Developmental neurotoxicity of industrial chemicals.  
673 *Lancet* **368**, 2167-2178 (2006).
- 674 2. Grandjean, P. & Landrigan, P.J. Neurobehavioural effects of developmental toxicity.  
675 *Lancet Neurol* **13**, 330-338 (2014).
- 676 3. Landrigan, P.J., *et al.* Neuropsychological dysfunction in children with chronic low-level  
677 lead absorption. *Lancet* **1**, 708-712 (1975).
- 678 4. Jacobson, J.L. & Jacobson, S.W. Intellectual impairment in children exposed to  
679 polychlorinated biphenyls in utero. *N Engl J Med* **335**, 783-789 (1996).
- 680 5. Nave, K.A. Myelination and the trophic support of long axons. *Nat Rev Neurosci* **11**, 275-  
681 283 (2010).
- 682 6. Giedd, J.N., *et al.* Brain development during childhood and adolescence: a longitudinal  
683 MRI study. *Nat Neurosci* **2**, 861-863 (1999).
- 684 7. Sanmarco, L.M., *et al.* Identification of environmental factors that promote intestinal  
685 inflammation. *Nature* (2022).
- 686 8. Wheeler, M.A., *et al.* Environmental Control of Astrocyte Pathogenic Activities in CNS  
687 Inflammation. *Cell* **176**, 581-596 e518 (2019).
- 688 9. Lidsky, T.I. & Schneider, J.S. Lead neurotoxicity in children: basic mechanisms and  
689 clinical correlates. *Brain* **126**, 5-19 (2003).
- 690 10. Li, Q., *et al.* Prevalence of Autism Spectrum Disorder Among Children and Adolescents  
691 in the United States From 2019 to 2020. *JAMA Pediatr* **176**, 943-945 (2022).
- 692 11. Chung, W., *et al.* Trends in the Prevalence and Incidence of Attention-  
693 Deficit/Hyperactivity Disorder Among Adults and Children of Different Racial and Ethnic  
694 Groups. *JAMA Netw Open* **2**, e1914344 (2019).
- 695 12. Zhou, T., *et al.* A hPSC-based platform to discover gene-environment interactions that  
696 impact human beta-cell and dopamine neuron survival. *Nat Commun* **9**, 4815 (2018).
- 697 13. Caporale, N., *et al.* From cohorts to molecules: Adverse impacts of endocrine disrupting  
698 mixtures. *Science* **375**, eabe8244 (2022).
- 699 14. Bercury, K.K. & Macklin, W.B. Dynamics and mechanisms of CNS myelination. *Dev Cell*  
700 **32**, 447-458 (2015).
- 701 15. Elitt, M.S., *et al.* Suppression of proteolipid protein rescues Pelizaeus-Merzbacher  
702 disease. *Nature* **585**, 397-403 (2020).
- 703 16. Chang, A., Tourtellotte, W.W., Rudick, R. & Trapp, B.D. Premyelinating oligodendrocytes  
704 in chronic lesions of multiple sclerosis. *N Engl J Med* **346**, 165-173 (2002).

- 705 17. Jakel, S., *et al.* Altered human oligodendrocyte heterogeneity in multiple sclerosis.  
706 *Nature* **566**, 543-547 (2019).
- 707 18. Breinlinger, S., *et al.* Hunting the eagle killer: A cyanobacterial neurotoxin causes  
708 vacuolar myelinopathy. *Science* **371**(2021).
- 709 19. Klose, J., *et al.* Neurodevelopmental toxicity assessment of flame retardants using a  
710 human DNT in vitro testing battery. *Cell Biol Toxicol* **38**, 781-807 (2022).
- 711 20. Silbereis, J.C., Pochareddy, S., Zhu, Y., Li, M. & Sestan, N. The Cellular and Molecular  
712 Landscapes of the Developing Human Central Nervous System. *Neuron* **89**, 248-268  
713 (2016).
- 714 21. Lager, A.M., *et al.* Rapid functional genetics of the oligodendrocyte lineage using  
715 pluripotent stem cells. *Nat Commun* **9**, 3708 (2018).
- 716 22. Najm, F.J., *et al.* Drug-based modulation of endogenous stem cells promotes functional  
717 remyelination in vivo. *Nature* **522**, 216-220 (2015).
- 718 23. Najm, F.J., *et al.* Rapid and robust generation of functional oligodendrocyte progenitor  
719 cells from epiblast stem cells. *Nat Methods* **8**, 957-962 (2011).
- 720 24. Richard, A.M., *et al.* ToxCast Chemical Landscape: Paving the Road to 21st Century  
721 Toxicology. *Chem Res Toxicol* **29**, 1225-1251 (2016).
- 722 25. Sommers, K.J., *et al.* Quaternary Phosphonium Compounds: An Examination of Non-  
723 Nitrogenous Cationic Amphiphiles That Evade Disinfectant Resistance. *ACS Infect Dis*  
724 **8**, 387-397 (2022).
- 725 26. Hora, P.I., Pati, S.G., McNamara, P.J. & Arnold, W.A. Increased Use of Quaternary  
726 Ammonium Compounds during the SARS-CoV-2 Pandemic and Beyond: Consideration  
727 of Environmental Implications. *Environ Sci Tech Lett* **7**, 622-631 (2020).
- 728 27. Madhavan, M., *et al.* Induction of myelinating oligodendrocytes in human cortical  
729 spheroids. *Nat Methods* **15**, 700-706 (2018).
- 730 28. Paşca, S.P., *et al.* A nomenclature consensus for nervous system organoids and  
731 assembloids. *Nature* **609**, 907-910 (2022).
- 732 29. Paul-Friedman, K., *et al.* Limited Chemical Structural Diversity Found to Modulate  
733 Thyroid Hormone Receptor in the Tox21 Chemical Library. *Environ Health Perspect* **127**,  
734 97009 (2019).
- 735 30. Liu, W., *et al.* Prenatal exposure to halogenated, aryl, and alkyl organophosphate esters  
736 and child neurodevelopment at two years of age. *J Hazard Mater* **408**, 124856 (2021).
- 737 31. Hoffman, K., Gearhart-Serna, L., Lorber, M., Webster, T.F. & Stapleton, H.M. Estimated  
738 tris(1,3-dichloro-2-propyl) phosphate exposure levels for US infants suggest potential  
739 health risks. *Environ Sci Technol Lett* **4**, 334-338 (2017).
- 740 32. Ciesielski, T., *et al.* Cadmium exposure and neurodevelopmental outcomes in U.S.  
741 children. *Environ Health Perspect* **120**, 758-763 (2012).
- 742 33. Kwon, S. & O'Neill, M. Socioeconomic and Familial Factors Associated with Gross Motor  
743 Skills among US Children Aged 3-5 Years: The 2012 NHANES National Youth Fitness  
744 Survey. *Int J Environ Res Public Health* **17**(2020).
- 745 34. Steadman, P.E., *et al.* Disruption of Oligodendrogenesis Impairs Memory Consolidation  
746 in Adult Mice. *Neuron* **105**, 150-164 e156 (2020).
- 747 35. McKenzie, I.A., *et al.* Motor skill learning requires active central myelination. *Science*  
748 **346**, 318-322 (2014).
- 749 36. Xiao, L., *et al.* Rapid production of new oligodendrocytes is required in the earliest  
750 stages of motor-skill learning. *Nat Neurosci* **19**, 1210-1217 (2016).
- 751 37. Edgar, N. & Sibille, E. A putative functional role for oligodendrocytes in mood regulation.  
752 *Transl Psychiatry* **2**, e109 (2012).
- 753 38. Kleinstreuer, N.C., *et al.* Phenotypic screening of the ToxCast chemical library to classify  
754 toxic and therapeutic mechanisms. *Nat Biotechnol* **32**, 583-591 (2014).

- 755 39. Zheng, G., Webster, T.F. & Salamova, A. Quaternary Ammonium Compounds:  
756 Bioaccumulation Potentials in Humans and Levels in Blood before and during the Covid-  
757 19 Pandemic. *Environ Sci Technol* **55**, 14689-14698 (2021).
- 758 40. United States Environmental Protection Agency: Disinfectants for Coronavirus (COVID-  
759 19); <https://www.epa.gov/coronavirus/about-list-n-disinfectants-coronavirus-covid-19-0>.
- 760 41. Lin, W. & Popko, B. Endoplasmic reticulum stress in disorders of myelinating cells. *Nat*  
761 *Neurosci* **12**, 379-385 (2009).
- 762 42. Li, D., Sangion, A. & Li, L. Evaluating consumer exposure to disinfecting chemicals  
763 against coronavirus disease 2019 (COVID-19) and associated health risks. *Environ Int*  
764 **145**, 106108 (2020).
- 765 43. Herron, J.M., *et al.* Multiomics Investigation Reveals Benzalkonium Chloride  
766 Disinfectants Alter Sterol and Lipid Homeostasis in the Mouse Neonatal Brain.  
767 *Toxicological Sciences* **171**, 32-45 (2019).
- 768 44. Patisaul, H.B., *et al.* Beyond Cholinesterase Inhibition: Developmental Neurotoxicity of  
769 Organophosphate Ester Flame Retardants and Plasticizers. *Environ Health Perspect*  
770 **129**, 105001 (2021).
- 771 45. Hou, M., Zhang, B., Fu, S., Cai, Y. & Shi, Y. Penetration of Organophosphate Triesters  
772 and Diesters across the Blood-Cerebrospinal Fluid Barrier: Efficiencies, Impact Factors,  
773 and Mechanisms. *Environ Sci Technol* **56**, 8221-8230 (2022).
- 774 46. Blum, A., *et al.* Organophosphate Ester Flame Retardants: Are They a Regrettable  
775 Substitution for Polybrominated Diphenyl Ethers? *Environ Sci Technol Lett* **6**, 638-649  
776 (2019).
- 777 47. Hou, M., Zhang, B., Fu, S., Cai, Y. & Shi, Y. Penetration of Organophosphate Triesters  
778 and Diesters across the Blood-Cerebrospinal Fluid Barrier: Efficiencies, Impact Factors,  
779 and Mechanisms. *Environmental Science & Technology* **56**, 8221-8230 (2022).
- 780 48. Gibson, E.A., *et al.* Flame retardant exposure assessment: findings from a behavioral  
781 intervention study. *J Expo Sci Environ Epidemiol* **29**, 33-48 (2019).
- 782 49. Najm, F.J., *et al.* Isolation of epiblast stem cells from preimplantation mouse embryos.  
783 *Cell Stem Cell* **8**, 318-325 (2011).
- 784 50. Allan, K.C., *et al.* Non-canonical Targets of HIF1a Impair Oligodendrocyte Progenitor  
785 Cell Function. *Cell Stem Cell* **28**, 257-272 e211 (2021).
- 786 51. Hubler, Z., *et al.* Accumulation of 8,9-unsaturated sterols drives oligodendrocyte  
787 formation and remyelination. *Nature* **560**, 372-376 (2018).
- 788 52. Bankhead, P., *et al.* QuPath: Open source software for digital pathology image analysis.  
789 *Sci Rep* **7**, 16878 (2017).
- 790 53. Patro, R., Duggal, G., Love, M.I., Irizarry, R.A. & Kingsford, C. Salmon provides fast and  
791 bias-aware quantification of transcript expression. *Nat Methods* **14**, 417-419 (2017).
- 792 54. Adamson, B., *et al.* A Multiplexed Single-Cell CRISPR Screening Platform Enables  
793 Systematic Dissection of the Unfolded Protein Response. *Cell* **167**, 1867-1882 e1821  
794 (2016).
- 795 55. Wong, Y.L., *et al.* eIF2B activator prevents neurological defects caused by a chronic  
796 integrated stress response. *Elife* **8**(2019).
- 797 56. Judson, R., *et al.* Analysis of the Effects of Cell Stress and Cytotoxicity on In Vitro Assay  
798 Activity Across a Diverse Chemical and Assay Space. *Toxicol Sci* **153**, 409 (2016).
- 799 57. Paul Friedman, K., *et al.* Utility of In Vitro Bioactivity as a Lower Bound Estimate of In  
800 Vivo Adverse Effect Levels and in Risk-Based Prioritization. *Toxicol Sci* **173**, 202-225  
801 (2020).
- 802



**Fig. 1**

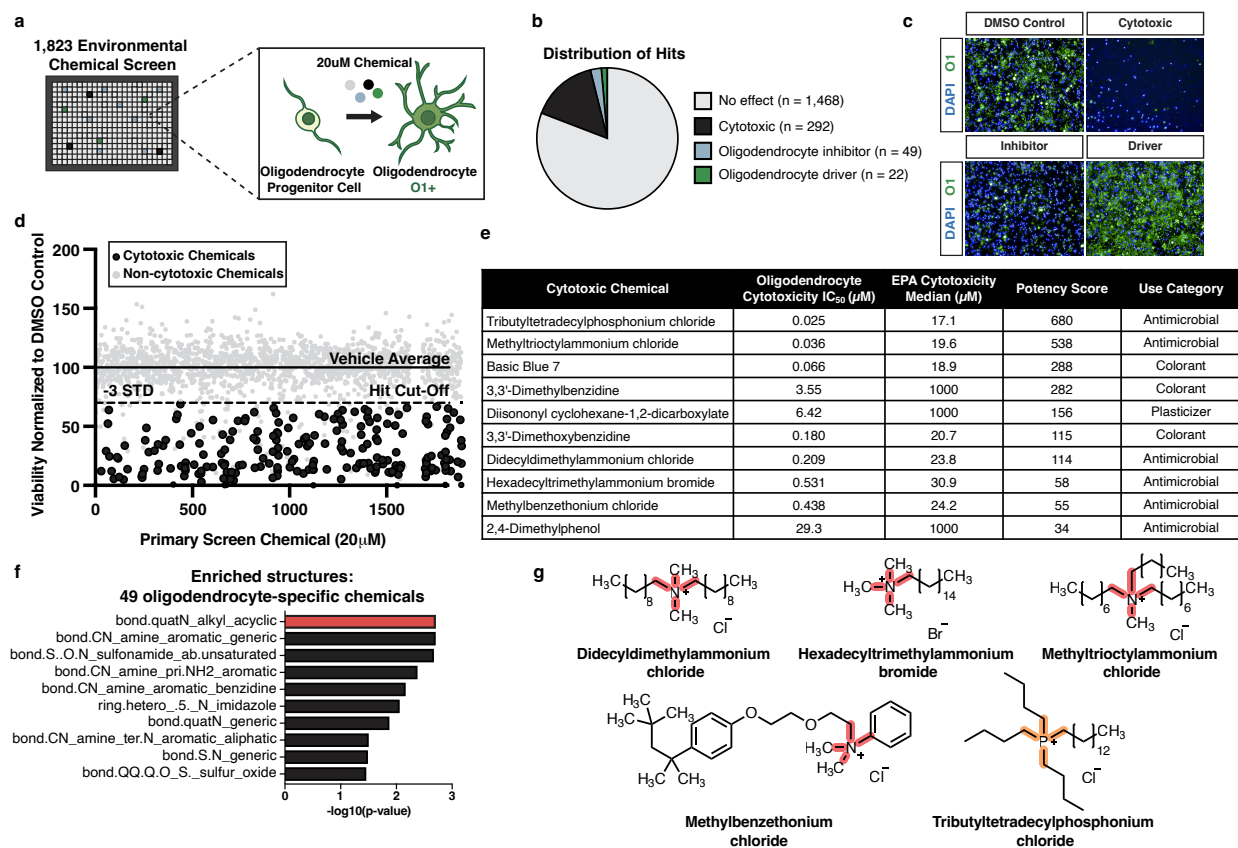


**Fig. 1: Quaternary compounds are potentially cytotoxic to developing oligodendrocytes.**

**a**, Schematic of the primary chemical screen in mPSC-derived oligodendrocytes.

**b**, Pie chart of the number of cytotoxic chemicals (black), inhibitors of oligodendrocyte development (blue), and drivers of oligodendrocyte development (green) identified from the primary chemical screen, along with chemicals that had no effect (gray).

**c**, Representative immunohistochemistry images after 3 days of oligodendrocyte development. Each image shows cells cultured with DMSO (vehicle control), or one of three chemicals with different effects on oligodendrocyte generation. Nuclei are marked using DAPI (in blue) and oligodendrocytes are marked using O1 (in green).

**d**, Primary chemical screen showing the effect of 1,823 environmental chemicals on the viability of developing oligodendrocytes displayed as viability normalized to vehicle control. The solid line represents the average of the vehicle control set at 100%. The dotted line marks a reduction in viability of 30% (>3 standard deviations). The 206 cytotoxic hits that pass this threshold and were validated by MTS are colored in black. Non-cytotoxic chemicals and cytotoxic hits not validated by MTS are colored in gray.

**e**, Table showing characteristics of 49 oligodendrocyte-specific cytotoxic hits tested in 10-point dose response from (40 nM to 20 μM). IC<sub>50</sub> values were determined with curve-fitting and compared to median cytotoxicity values obtained from the EPA database for each chemical. Potency scores were calculated by dividing the cytotoxicity median by the



experimentally determined IC50 in oligodendrocytes. Chemicals were ranked based on increasing potency score. Table also includes each chemical's use category.

**f**, Chemotype analysis for the 49 oligodendrocyte-specific cytotoxic compounds, with the most enriched structural domain, bond.quatN\_alkyl\_acyclic (p-value = 0.002, OR = 16.2), highlighted in red. p-values were generated using a one-sided Fisher's exact test.

**g**, Chemical structures for the four quaternary ammonium compounds and one quaternary phosphonium compound. The enriched cytotoxicity-associated bond for quaternary ammonium compounds is highlighted in red. The quaternary phosphonium bond is highlighted in orange.

**Fig. 2**

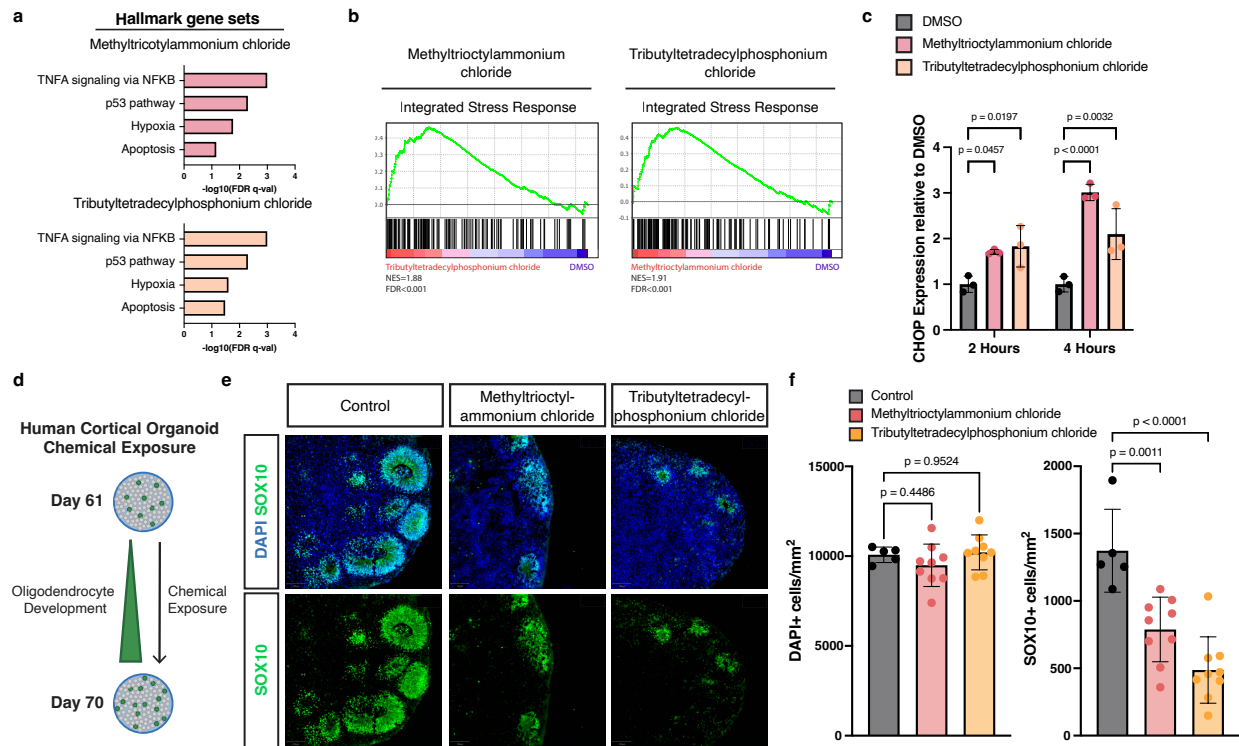


**Fig. 2: Quaternary compounds activate the integrated stress response and are cytotoxic to human oligodendrocytes.**

**a**, Gene set enrichment analysis (GSEA) of hallmark gene sets upregulated in OPCs in response to incubation with 20  $\mu$ M quaternary ammonium (red) or phosphonium compounds (orange) for 4 hours.

**b**, GSEA of an integrated stress response gene set in OPCs treated with methyltrioctylammonium chloride or tributyltetradecylphosphonium chloride compared with DMSO treated OPCs demonstrates significant enrichment (FDR<0.001) for genes involved in the integrated stress response (normalized enrichment scores [NES] = 1.91, 1.88 respectively).

**c**, qRT-PCR of CHOP in OPCs treated with DMSO (gray), methyltrioctylammonium chloride (red), and tributyltetradecylphosphonium chloride (orange). Data are presented as the mean value  $\pm$  standard deviation from three biological replicates, represented as closed circles. P values were calculated using one-way ANOVA with Dunnett post-test correction for multiple comparisons.

**d**, Schematic depicting exposure of human cortical organoids to cytotoxic chemicals.

**e**, Representative immunohistochemistry images of control human cortical organoids and organoids treated for 10 days with 360 nM methyltrioctylammonium chloride or 300 nM tributyltetradecylphosphonium chloride (approximate IC<sub>90</sub> in mPSC-derived oligodendrocytes). Images show all cells (DAPI+, blue) and oligodendrocytes (SOX10+, in green) at day 70.

**f**, Quantification of total cell number (DAPI+ per mm<sup>2</sup>) and oligodendrocytes (SOX10+ per mm<sup>2</sup>) in the whole cortical organoid. Data are presented as the mean value  $\pm$  standard deviation from  $n \geq 5$  biological replicates (individual organoids) indicated by

closed circle data points. p-values were calculated using one-way ANOVA with Dunnett post-test correction for multiple comparisons.

**Fig. 3**

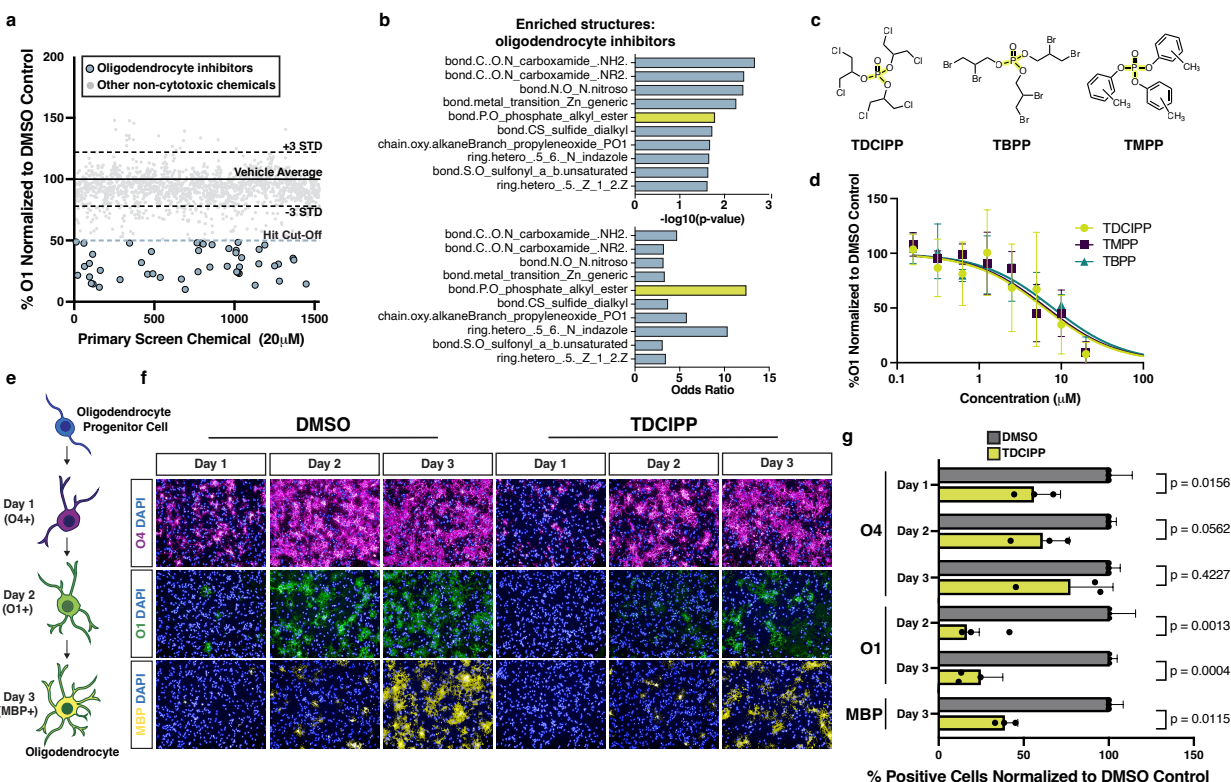


**Fig. 3: Organophosphate flame retardants arrest oligodendrocyte maturation.**

**a**, Primary chemical screen showing the effect of 1,539 non-cytotoxic environmental chemicals on oligodendrocyte development displayed as percent O1+ cells normalized to DMSO. The dotted lines mark  $\pm 3$  standard deviations from the mean of control wells. The blue dotted line marks the inhibitor hit cutoff, a reduction in O1+ cells of 50% ( $>7$  standard deviations) compared to DMSO. The 49 oligodendrocyte inhibitors that pass this threshold are colored in blue. All other non-cytotoxic chemicals that did not inhibit oligodendrocyte development are colored in gray.

**b**, Chemotype analysis for oligodendrocyte inhibitors showing both the p-value and odds ratio. Among the top most significant structural domains, bond.P.O\_phosphate\_alkyl\_ester (p-value = 0.02, OR = 12.5) has the highest odds ratio, and is highlighted in yellow. p-values were generated using a one-sided Fisher's exact test.

**c**, Chemical structures for three organophosphate flame retardants containing the structure bond.P.O\_phosphate\_alkyl\_ester, highlighted in yellow.

**d**, Graph of eight-point dose response (30 nM to 20  $\mu$ M) quantifying the effect of three organophosphate flame retardants on oligodendrocyte (O1+) generation from OPCs. Data are presented as the mean value  $\pm$  standard deviation from three biological replicates (OPC batches generated from independent mPSC lines).

**e**, Schematic showing stages of in vitro oligodendrocyte development and the markers for early (O4), intermediate (O1), and late (MBP) oligodendrocytes.

**f**, Representative images of early (O4+, in magenta), intermediate (O1+, in green), and late (MBP+ in yellow) oligodendrocytes after treatment with DMSO vehicle control or 20  $\mu$ M TDCIPP for 1, 2, and 3 days of maturation. Nuclei are marked using DAPI (in blue). Images for oligodendrocytes treated with TMPP and TBPP are shown in Extended Data Fig. 4e.

**g**, Quantification of early (O4+), intermediate (O1+), and late (MBP+) oligodendrocytes, after day 1, 2, and 3 of development, normalized to DMSO vehicle control. Data are presented as the mean value  $\pm$  standard deviation from three biological replicates (OPC batches generated from independent mPSC lines), indicated by closed circle data points. Data for oligodendrocytes treated with TBPP and TMPP are shown in Extended Data Fig. 4f. p-values were calculated using one-way ANOVA with Dunnett post-test correction for multiple comparisons.



**Fig. 4**

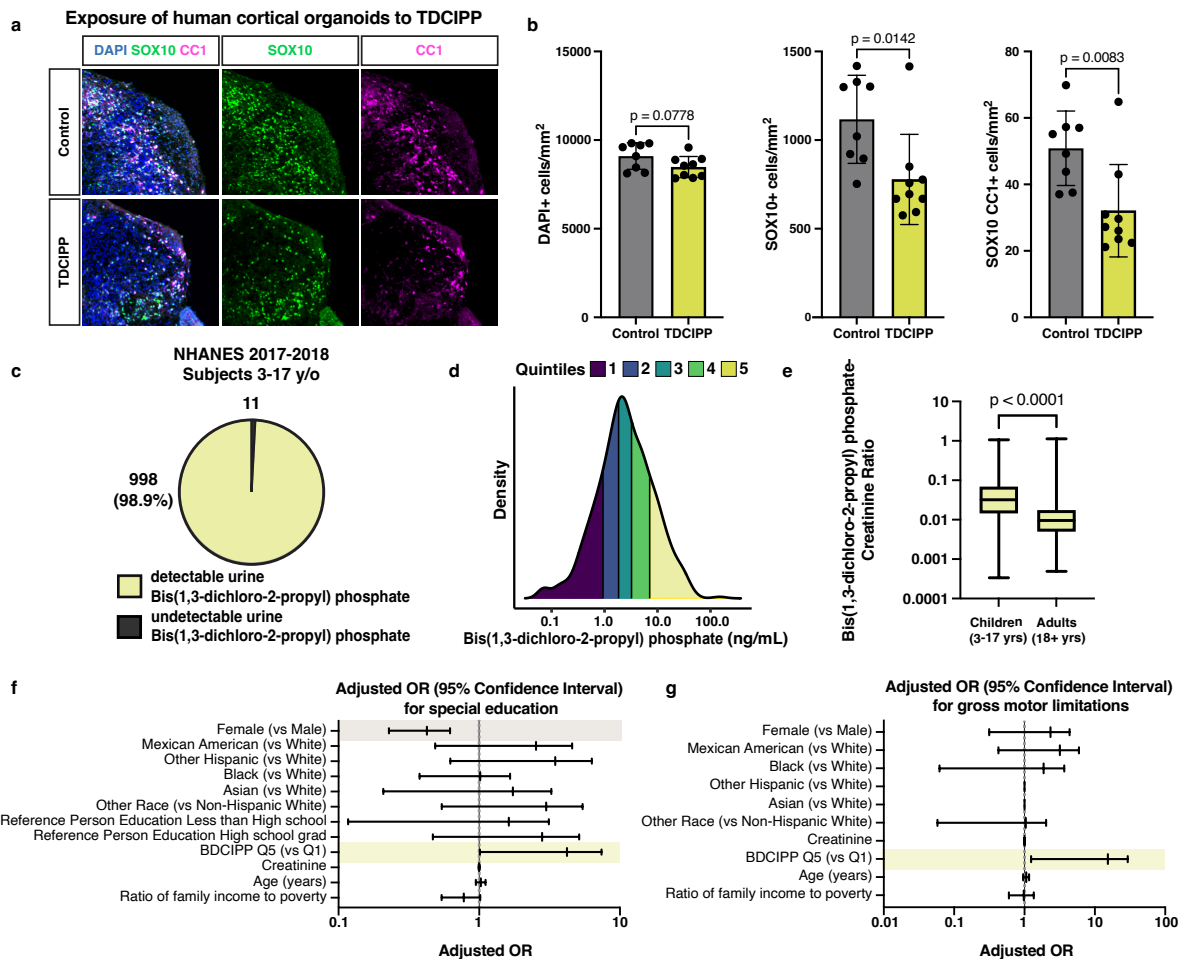


**Fig. 4: TDCIPP inhibits human oligodendrocyte development and is associated with abnormal neurodevelopmental outcomes in children.**

**a**, Representative immunohistochemistry images of human cortical organoids treated for 10 days with the flame retardant TDCIPP at 18  $\mu$ M (approximate IC75 in mPSC-derived oligodendrocytes). Images show all cells (DAPI+, in blue), oligodendrocyte lineage cells (SOX10+, in green), and oligodendrocytes (CC1+, in magenta).

**b**, Quantification of total cell number (DAPI+ per mm<sup>2</sup>), oligodendrocyte lineage cells (SOX10+ per mm<sup>2</sup>) and mature oligodendrocytes (SOX10+CC1+ per mm<sup>2</sup>) in whole cortical organoids. Data are presented as the mean value  $\pm$  standard deviation from  $n \geq 8$  biological replicates (individual organoids) indicated by closed circle data points for TDCIPP-treated organoids. p-values were calculated using Student's two-tailed t test.

**c**, Pie chart showing the number of children ages 3-17 years old from the NHANES 2017-2018 dataset with undetectable and detectable levels of BDCIPP, the urine metabolite of TDCIPP.

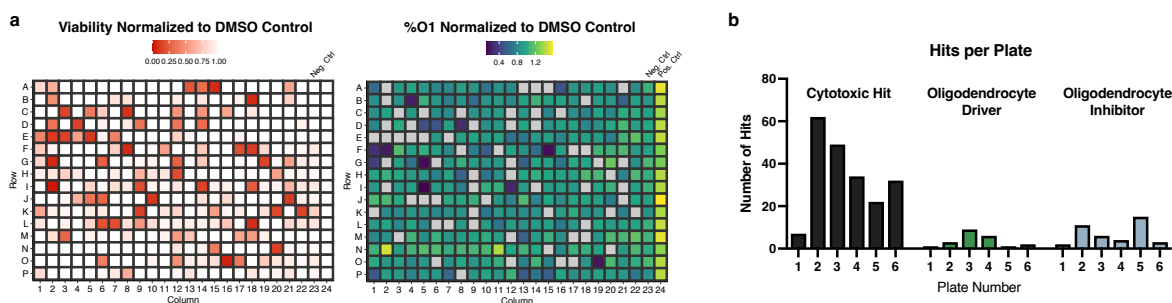
**d**, Density plot showing the range and quintiles of urine BDCIPP levels in children ages 3-17 years old from the NHANES 2017-2018 dataset.

**e**, Boxplot showing creatinine-normalized levels of BDCIPP in children 3-17 years of age and adults aged 18 years and older. p-value was calculated using the Kruskal Wallis one-way ANOVA.

**f**, Adjusted odds ratio for the neurodevelopmental outcome: requiring special education or early intervention. Significant odds ratios are highlighted in yellow (BDCIPP Q5 v Q1 OR = 2.7 [95% CI = 1.012-7.407) and gray (Female v Male OR = 0.376 [95% CI = 0.228-0.621]).

**g**, Adjusted odds ratio for the neurodevelopmental outcome: gross motor limitations. Significant odds ratios are highlighted in yellow (BDCIPP Q5 v Q1 OR = 6.0 [95% CI = 1.243-29.426]).

## Extended Data Figure 1

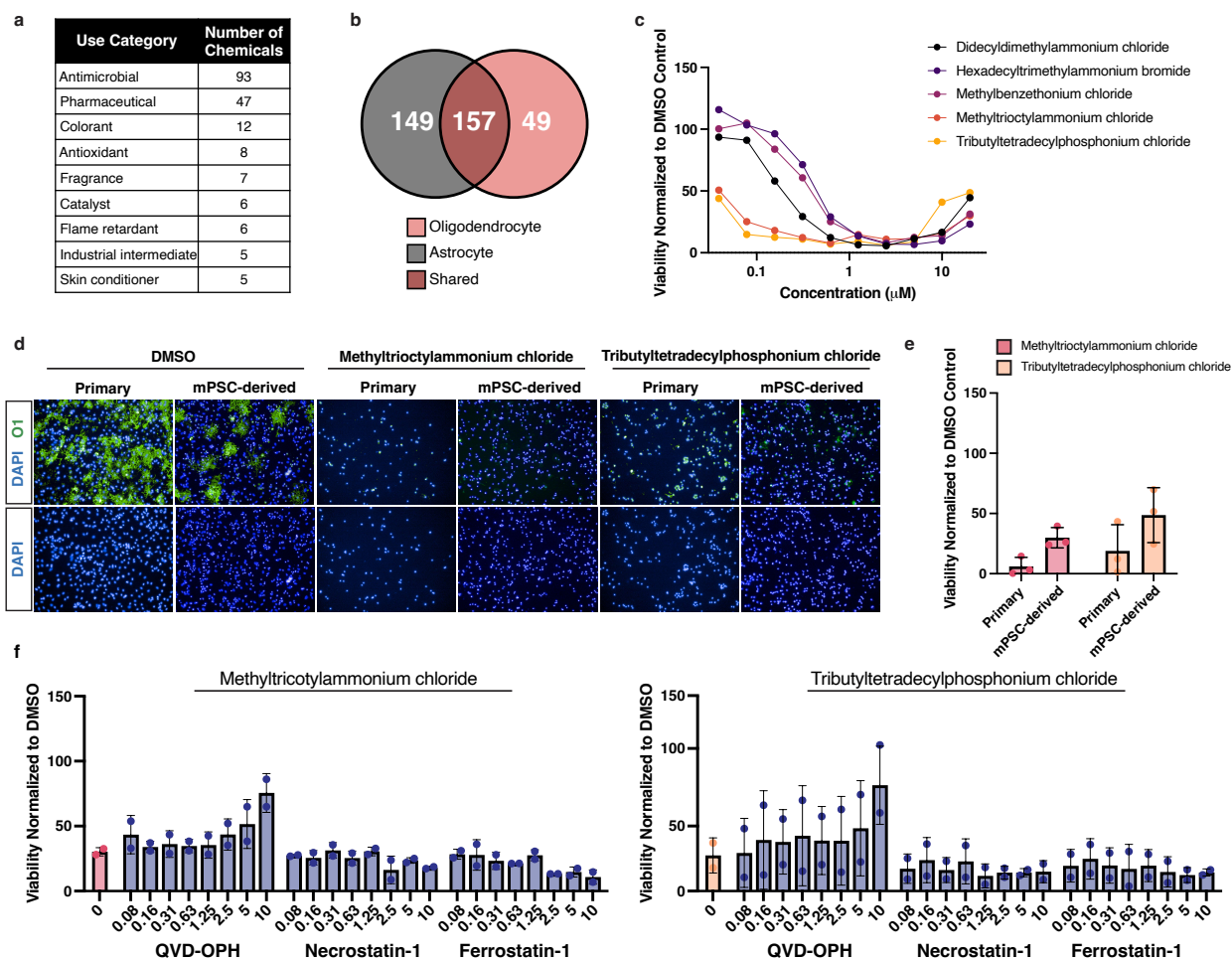


### Extended Data Fig. 1: Screening a library of environmental chemicals in developing oligodendrocytes identifies cytotoxic chemicals and modulators of oligodendrocyte generation.

**a**, Representative heatmaps of one of six primary screening 384-well plates depicting cytotoxic compounds (red), oligodendrocyte inhibitors (blue), and drivers (green). Viability and percent O1+ oligodendrocytes are normalized to vehicle control (DMSO). Thyroid hormone, a known driver of oligodendrocyte generation, is included as a positive control for oligodendrocyte development.

**b**, Quantification of hits across 6 primary screening plates showing distribution of chemicals identified as cytotoxic (black), drivers (green), and inhibitors (blue).

## Extended Data Fig. 2



### Extended Data Fig. 2: Quaternary compounds are specifically cytotoxic to oligodendrocyte development and induce apoptosis.

**a**, Table of the top use categories for the 206 validated cytotoxic chemicals and the number of chemicals belonging to each category.

**b**, Venn diagram showing the overlap of 206 validated cytotoxic chemicals identified in the oligodendrocyte screen (in red) compared to cytotoxic hits identified in an identical screen performed in mouse astrocytes (in gray).

**c**, Quaternary compounds tested in 10-point dose response from (40 nM to 20  $\mu$ M), on developing oligodendrocytes quantifying cell number (DAPI+). Data are presented as the mean value from 3 biological replicates (OPC batches generated from independent mPSC lines).

**d**, Representative immunohistochemistry images of mPSC-derived oligodendrocytes (O1+, in green) and primary mouse oligodendrocytes treated with methyltrioctylammonium chloride and tributyltetradecylphosphonium chloride. Nuclei are marked by DAPI (in blue).

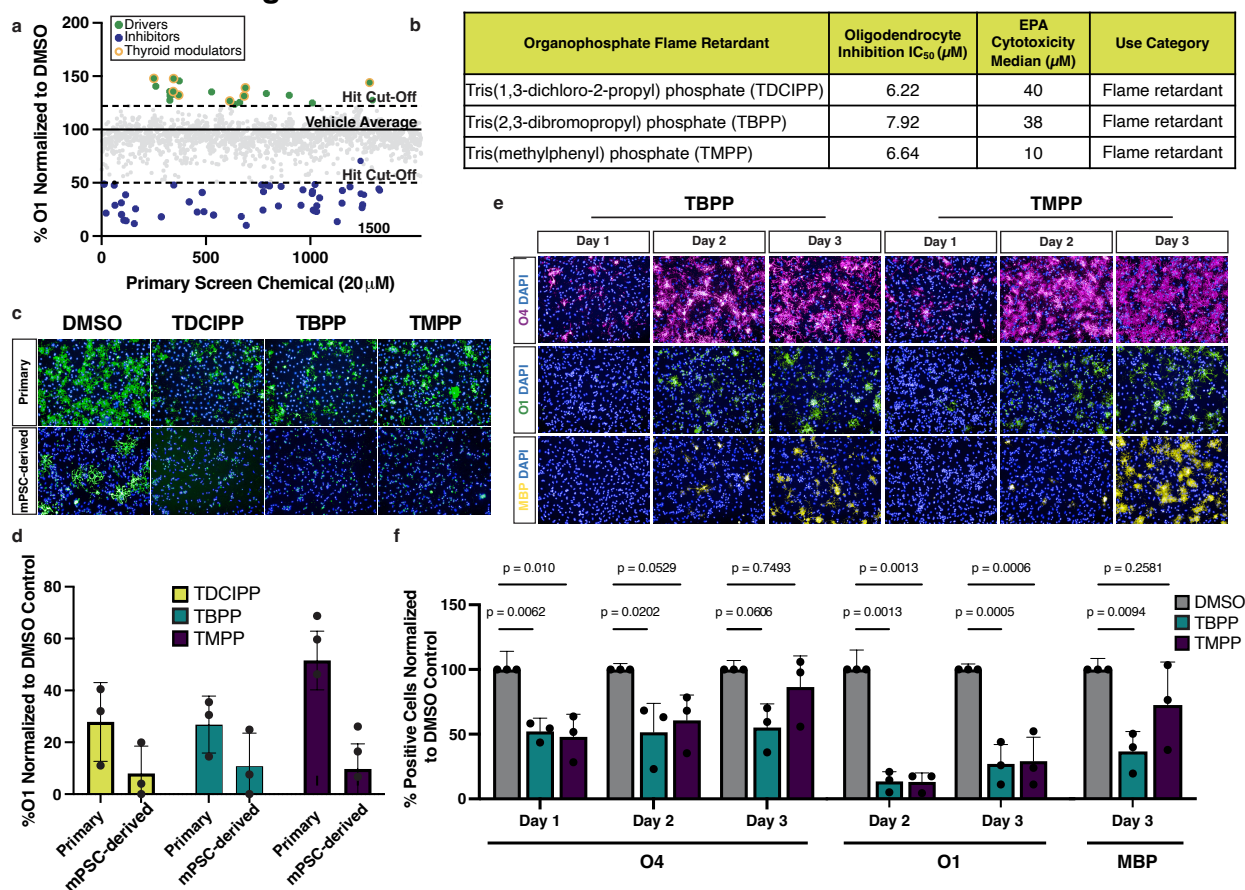
**e**, Quantification of viability of mouse primary and PSC-derived oligodendrocytes treated with 20  $\mu$ M methyltrioctylammonium chloride or tributyltetradecylphosphonium chloride. Data are presented as the mean  $\pm$  standard deviation from three biological replicates,

represented by closed circles (from independent primary OPC isolations or OPC batches from independent mPSC lines).

**f**, Quantification of oligodendrocyte viability normalized to DMSO control. Developing oligodendrocytes were cultured for 3 days in the presence of 120 nM methyltrioctylammonium chloride or 100 nM tributyltetradecylphosphonium chloride at (approximate IC75 in mPSC-derived OPCs), and cell death inhibitors QVD-OPH, necrostatin-1, and ferrostatin-1, in 8-point dose response (80 nM to 10  $\mu$ M). Data are presented as the mean  $\pm$  standard deviation from two biological replicates, represented by closed circles (OPC batches generated from independent mPSC lines).



## Extended Data Fig. 3



## Extended Data Fig. 3: Organophosphate flame retardants inhibit oligodendrocyte development.

**a**, Primary chemical screen of 1,539 non-cytotoxic environmental chemicals showing the effect of individual chemicals on oligodendrocyte generation, presented as percent O1+ cells normalized to the DMSO control, as shown in Fig. 2a. Two dotted lines show the hit cutoffs for identification of oligodendrocyte drivers and inhibitors. Drivers result in an increase of O1+ percentage by 22% (>3 standard deviations) compared to negative DMSO control. Inhibitors reduce O1+ percentage by more than 50% (>7 standard deviations) compared to negative DMSO control. Thyroid modulators are highlighted in yellow.

**b**, Table shows IC<sub>50</sub> concentrations, cytotoxicity median values, and use categories for three organophosphate esters identified as inhibitors of oligodendrocyte development.

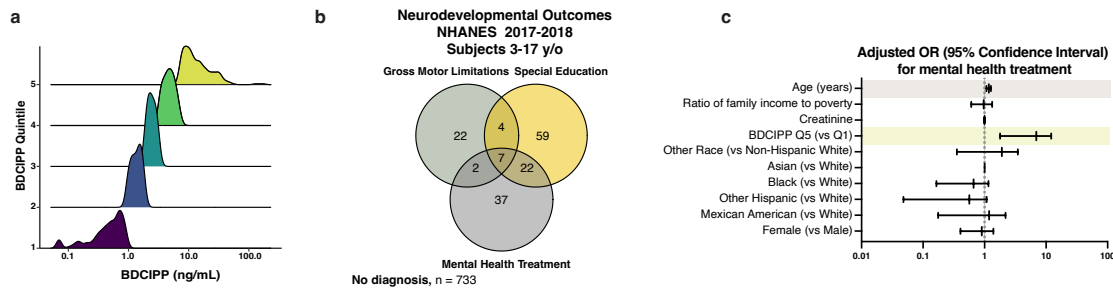
**c**, Representative immunohistochemistry images of oligodendrocytes, generated from mPSC-derived OPCs and mouse primary OPCs, tested with three organophosphate flame retardants at 20 μM. Generation of oligodendrocytes was evaluated using the oligodendrocyte marker O1 (green). Nuclei are marked with DAPI (in blue).

**d**, Quantification O1+ mPSC-derived and primary oligodendrocytes, shown as a percentage of DAPI+ cell number, across three biological replicates, represented at closed circles (independent isolations of primary OPCs and OPC batches generated from independent mPSC lines).

**e**, Immunohistochemistry images of early (O4+, in magenta), intermediate (O1+, in green), and late (MBP+, in yellow) oligodendrocytes treated with 20  $\mu$ M TBPP or TMPP. Control images and TDCIPP treated oligodendrocytes are shown in Fig. 2e. Nuclei are marked with DAPI (in blue).

**f**, Quantification of primary oligodendrocytes at the early (O4+), intermediate (O1+), and late (MBP+) stage, shown as a percentage of DAPI+ cell number, over three days of development. Data are presented as the mean  $\pm$  standard deviation from three biological replicates (OPC batches generated from independent mPSC lines), indicated by closed circle data points. p-values were calculated using one-way ANOVA with Dunnett post-test correction for multiple comparisons.

## Extended Data Fig. 4



### Extended Data Fig. 4: TDCIPP is associated with abnormal neurodevelopmental outcomes in children.

**a**, Venn diagram showing co-occurrence of three neurodevelopmental outcomes in the study population.

**b**, Density plots showing the distribution of urine BDCIPP levels within individual quintiles.

**c**, Adjusted odds ratio for the neurodevelopmental outcome “sought mental health treatment”. Significant odds ratios are highlighted in blue (BDCIPP Q5 v Q1 OR = 4.6 [95% CI = 1.785-12.104) and significant covariates are highlighted in gray ( $p < 0.001$ ).

## **Supplementary Information Tables (provided as separate .xlsx files)**

### **Supplementary Table 1. Primary screening results**

Primary screening results showing the effects of environmental chemicals on the viability and generation of developing oligodendrocytes. Cytotoxic chemicals, identified by comparing DAPI-positive cell number in treated wells to vehicle (DMSO), are included in an additional sheet. Non-cytotoxic chemicals were assessed for effects on oligodendrocyte development. Chemicals that increased or decreased oligodendrocyte number, measured by the percentage of O1-positive oligodendrocytes, were identified as drivers or inhibitors, and are included in separate sheets.

### **Supplementary Table 2. ToxPrint enrichment analysis**

Computational analysis showing cytotoxicity-associated structures assigned to all chemicals in the 1,823 chemical library, and additional sheets for enriched structures within the top cytotoxic hits and inhibitors or oligodendrocyte development.

### **Supplementary Table 3. Expression data for quaternary compound treated OPCs**

Gene set enrichment results for OPCs treated with methyltrioctylammonium chloride or tributyltetradecylphosphonium chloride for 4 hours at IC<sub>90</sub> concentrations.